

Supplementary materials for “**Single-Crystal X-ray Diffraction on the Structure of (Al,Fe)-  
bearing Bridgmanite in the Lower Mantle**”

Suyu Fu<sup>1,2,\*</sup>, Stella Chariton<sup>3</sup>, Yanyao Zhang<sup>1</sup>, Takuo Okuchi<sup>4</sup>, Vitali B. Prakapenka<sup>3</sup>, Jung-  
Fu Lin<sup>1,\*</sup>

<sup>1</sup>Department of Geological Sciences, Jackson School of Geosciences, The University of Texas  
at Austin, Austin, TX, USA

<sup>2</sup>Department of Earth and Planetary Science, The University of Tokyo, Tokyo, Japan

<sup>3</sup>Center for Advanced Radiation Sources, The University of Chicago, Chicago, IL, USA

<sup>4</sup>Institute for Integrated Radiation and Nuclear Science, Kyoto University, Kyoto, Japan.

\*Corresponding author: Suyu Fu ([fsyxhy@gmail.com](mailto:fsyxhy@gmail.com)), Jung-Fu Lin ([afu@jsg.utexas.edu](mailto:afu@jsg.utexas.edu))

This document contains supplementary materials for the single-crystal x-ray diffraction  
results on bridgmanite at high pressure:

Figures S1-S5

Tables S1-S2

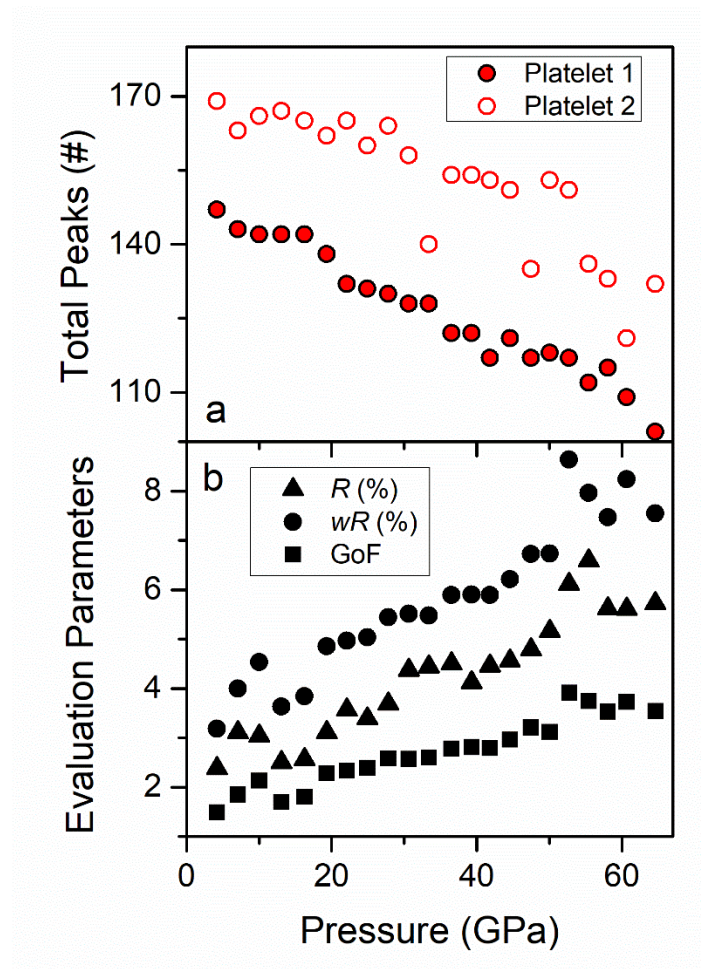


**Figure S1.** Data analyses on single-crystal X-ray diffraction patterns of Fe10-Al14-Bgm at high pressure. **a** The number of high-quality reflection peaks of each bridgmanite platelet used for structure refinements. These reflections were selected with intensities ( $I$ ) of  $I > 3\sigma(I)$ . Solid and open red circles are for platelets 1 and 2, respectively. **b** Evaluation parameters during the structure refinements on Fe10-Al14-Bgm using JANA software (Petříček et al. 2014). Circles: weighted  $R$ -factor ( $wR(F^2)$ ) in percentage; triangles:  $R$ -factor ( $R(F^2 > 2\sigma(F^2))$ ) in percentage; squares: goodness of fit (GoF).

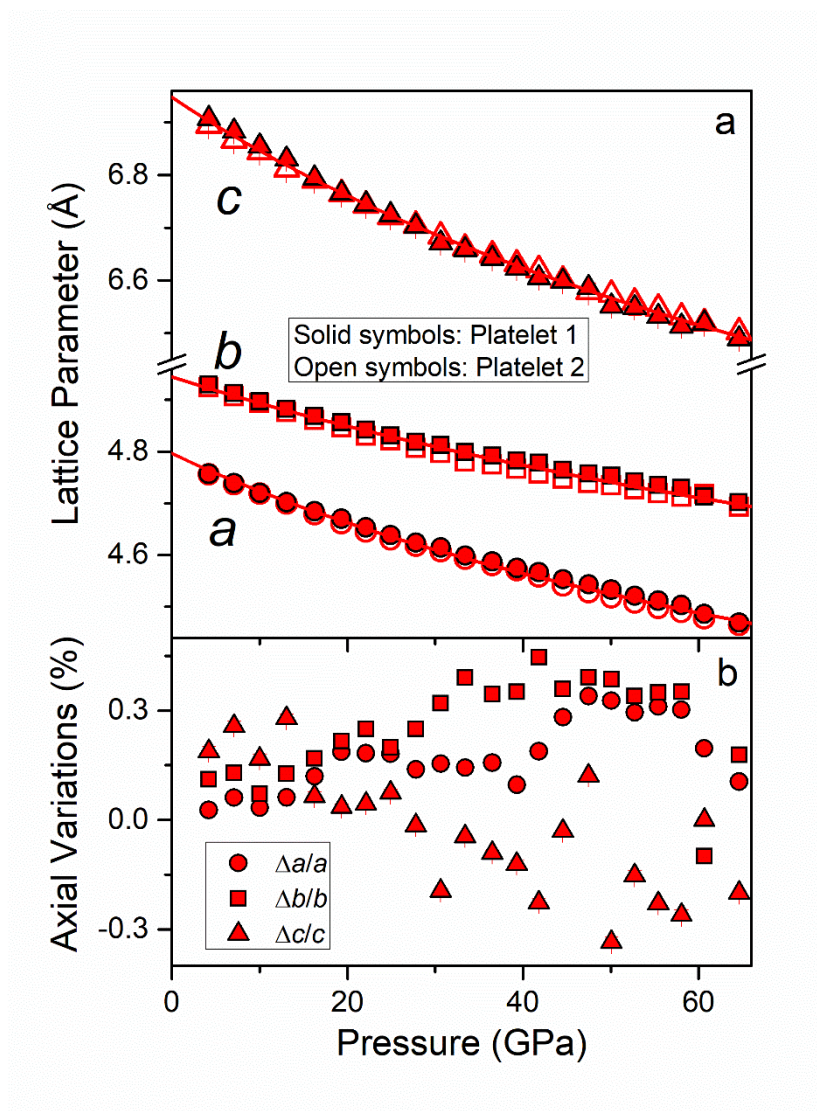


**Figure S2.** Lattice parameters of the two single-crystal Fe<sub>10</sub>-Al<sub>14</sub>-Bgm platelets obtained from analyses using CrysAlisPro software. **a** Lattice parameters (*a*, *b*, *c*) as a function of pressure. Solid and open symbols are for platelets 1 and 2, respectively. The solid lines are best fits to the dataset together using axial equation of state. **a** Axial variation (%) between the two platelets. Overall, the differences of the derived lattice parameters between the two platelets are less than 0.3%.

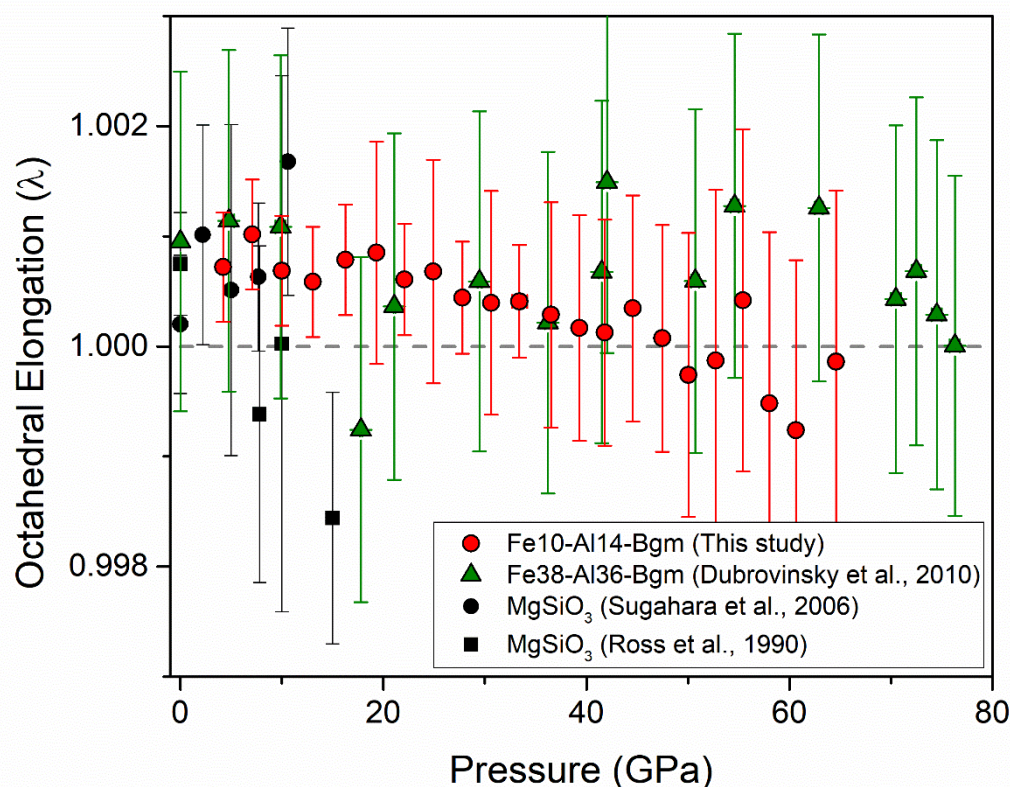


**Figure S3.** Octahedral elongation parameter ( $\lambda$ ) of the single-crystal Fe10-Al14-Bgm as a function of pressure.  $\lambda$  is calculated by following a previous study (Robinson et al. 1971):  $\lambda = \sum_{i=1}^6 (l_i/l_0)^2/6$ , where  $l_i$  and  $l_0$  are B-O bond lengths under strained and unstrained states, respectively. Red circles are results from this study, and literature reports on bridgmanite with different compositions are plotted for comparisons (Ross and Hazen 1990; Sugahara et al. 2006; Dubrovinsky et al. 2010; Boffa Ballaran et al. 2012). The dashed gray line has a  $\lambda$  value of 1, indicating an ideal octahedron.



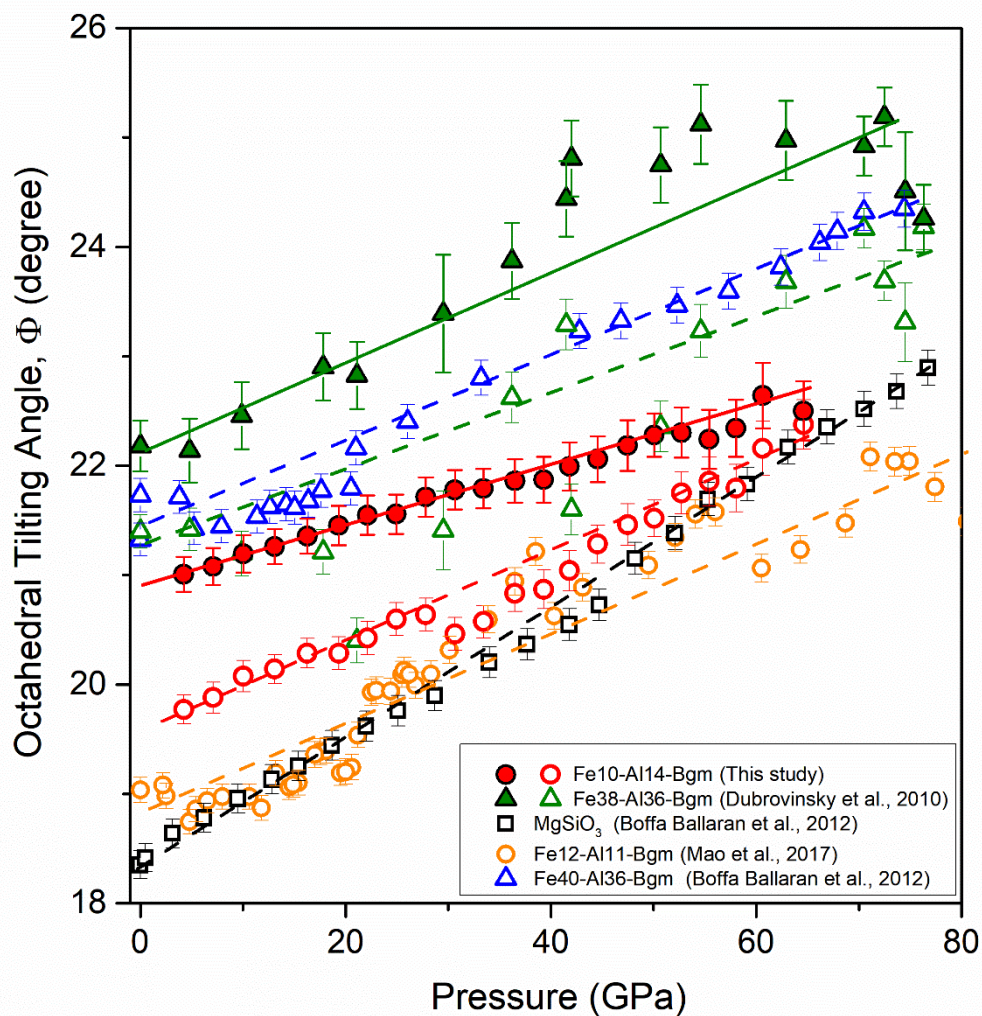


**Figure S4.** Octahedral titling angles in the single-crystal Fe10-Al14-Bgm as a function of pressure. Red circles are results of Fe10-Al14-Bgm in this study, and literature reports on bridgmanite with different compositions were plotted for comparisons (Dubrovinsky et al. 2010; Boffa Ballaran et al. 2012; Mao et al. 2017). Solid symbols are derived from the quantitatively refined atomic, while open symbols are calculations from unit-cell lattice parameters.

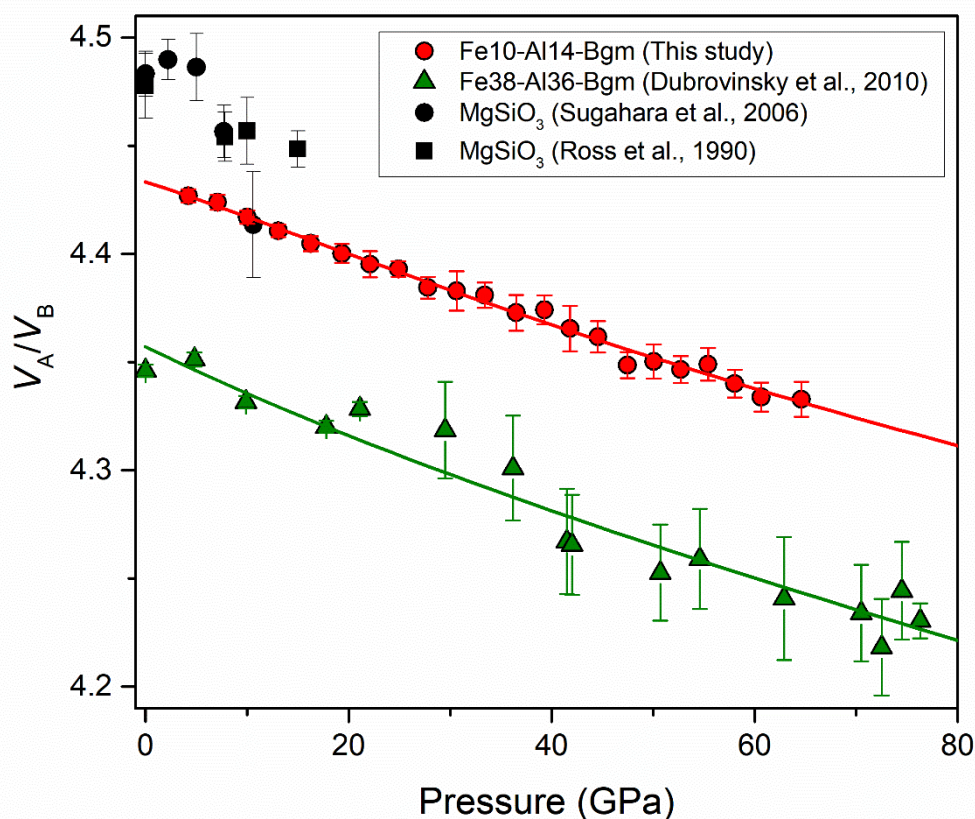


**Figure S5.** Volume ratios ( $V_A/V_B$ ) between the  $AO_{12}$  pseudo-dodecahedra and  $BO_6$  octahedra of Fe10-Al14-Bgm at high pressure. Red circles are results from this study, and literature reports on bridgmanite with different compositions are plotted for comparisons (Ross and Hazen 1990; Sugahara et al. 2006; Dubrovinsky et al. 2010; Boffa Ballaran et al. 2012). The lines are calculated from best-fits to volumes of  $AO_{12}$  pseudo-dodecahedra and  $BO_6$  octahedra using the Birch-Murnaghan equation.

**Table S1.** Refined unit-cell parameters of single-crystal Fe10-Al14-Bgm at high pressures. Au was used as a pressure calibrant. 1 $\sigma$  uncertainty was shown in parentheses.

Pressure (GPa)	<i>a</i> (Å)	<i>b</i> (Å)	<i>c</i> (Å)
4.2(1)	4.7564(11)	4.9266(3)	6.9005(19)
7.1(2)	4.7378(4)	4.9098(3)	6.8742(13)
10.0(2)	4.7191(4)	4.8949(4)	6.8492(14)
13.1(2)	4.7007(4)	4.8792(4)	6.8205(15)
16.3(2)	4.6816(4)	4.8648(4)	6.7918(17)
19.3(2)	4.6658(5)	4.8512(4)	6.7650(18)
22.1(3)	4.6491(4)	4.8362(4)	6.7435(19)
24.9(3)	4.6342(5)	4.8257(4)	6.722(3)
27.8(3)	4.6208(4)	4.8127(4)	6.703(2)
30.6(3)	4.6107(5)	4.8047(5)	6.677(3)
33.4(7)	4.5955(6)	4.7895(5)	6.660(2)
36.5(4)	4.5835(12)	4.7832(11)	6.645(4)
39.3(4)	4.5725(14)	4.7743(40)	6.627(5)
41.8(4)	4.5624(47)	4.7674(14)	6.612(5)
45.6(5)	4.5467(6)	4.7557(5)	6.599(5)
47.5(5)	4.5353(7)	4.7480(6)	6.582(5)
50.1(4)	4.5254(12)	4.7435(45)	6.562(6)
52.7(4)	4.5142(9)	4.7341(9)	6.553(6)
55.4(5)	4.5044(8)	4.7269(7)	6.540(6)
58.0(5)	4.4962(10)	4.7206(9)	6.522(6)
60.6(6)	4.4814(8)	4.7150(7)	6.519(6)
64.6(6)	4.4668(7)	4.6972(6)	6.496(6)

**Table S2.** The values of evaluation parameters ( $wR$  and GoF) in different models with a certain amount of Fe fixed in the B site during single-crystal refinements at the lowest experimental pressure of 4.2 GPa.

	A-site Fe ions (mol%)	B-site Fe ions (mol%)	A-site Al <sup>3+</sup> (mol%)	B-site Al <sup>3+</sup> (mol%)	$wR$ value (%)	GoF
Model 1(best- fit)	10	0	3	11	3.2	1.49
Model 2	5 (fixed)	5 (fixed)	8	6	11.6	4.38
Model 3	0 (fixed)	10 (fixed)	13	1	22.4	8.67



## References:

- Boffa Ballaran, T., Kurnosov, A., Glazyrin, K., Frost, D.J., Merlini, M., Hanfland, M., and Caracas, R. (2012) Effect of chemistry on the compressibility of silicate perovskite in the lower mantle. *Earth and Planetary Science Letters*, 333, 181–190.
- Dubrovinsky, L., Boffa-Ballaran, T., Glazyrin, K., Kurnosov, A., Frost, D., Merlini, M., Hanfland, M., Prakapenka, V.B., Schouwink, P., and Pippinger, T. (2010) Single-crystal X-ray diffraction at megabar pressures and temperatures of thousands of degrees. *High Pressure Research: Application to Earth Planetary Sciences*, 30, 620–633.
- Mao, Z., Wang, F., Lin, J.-F., Fu, S., Yang, J., Wu, X., Okuchi, T., Tomioka, N., Prakapenka, V.B., and Xiao, Y. (2017) Equation of state and hyperfine parameters of high-spin bridgmanite in the Earth's lower mantle by synchrotron X-ray diffraction and Mössbauer spectroscopy. *American Mineralogist*, 102, 357–368.
- Petríček, V., Dušek, M., and Palatinus, L. (2014) Crystallographic computing system JANA2006: general features. *Zeitschrift für Kristallographie-Crystalline Materials*, 229, 345–352.
- Robinson, K., Gibbs, G.V., and Ribbe, P.H. (1971) Quadratic Elongation: A Quantitative Measure of Distortion in Coordination Polyhedra. *Science*, 172, 567–570.
- Ross, N.L., and Hazen, R.M. (1990) High-pressure crystal chemistry of MgSiO<sub>3</sub> perovskite. *Physics and Chemistry of Minerals*, 17, 228–237.
- Sugahara, M., Yoshiasa, A., Komatsu, Y., Yamanaka, T., Bolfan-Casanova, N., Nakatsuka, A., Sasaki, S., and Tanaka, M. (2006) Reinvestigation of the MgSiO<sub>3</sub> perovskite structure at high pressure. *American Mineralogist*, 91, 533–536.